



Geophysical Research Letters

Supporting Information for

Weakening of the extratropical storm tracks in idealized solar geoengineering scenarios

**Charles G. Gertler¹, Paul A. O’Gorman¹, Ben Kravitz^{2,3}, John C. Moore^{4,5}, Steven J. Phipps⁶,
Shingo Watanabe⁷**

¹ Department of Earth, Atmospheric and Planetary Sciences, Massachusetts Institute of Technology, Cambridge, MA 02139

² Department of Earth and Atmospheric Sciences, Indiana University, Bloomington, IN 47408

³ Atmospheric Sciences and Global Change Division, Pacific Northwest National Laboratory, Richland, WA 99352

⁴ College of Global Change and Earth System Science, Beijing Normal University, Beijing 100875, China

⁵ Arctic Centre, University of Lapland, Rovaniemi, Finland

⁶ Institute for Marine and Antarctic Studies, University of Tasmania, Hobart, TAS 7001, Australia

⁷ Japan Agency for Marine-Earth Science and Technology (JAMSTEC), Yokohama, Japan

Contents of this file

Text S1

Figures S1 to S13

Table S1 to S2

Introduction

This supporting information contains one text section, 13 figures referenced in the main text and the supporting information, and two tables. The text section compares extratropical cyclone activity (ECA) and eddy kinetic energy (EKE), two metrics of storm track strength, in the one model for which sufficient data is available to make the comparison.

Text S1: Different storm track measures in one model

Eddy kinetic energy (EKE) has been used as a metric for storm track intensity in most studies that compare mean available potential energy (MAPE) and storm track intensity (e.g. O’Gorman (2010)). Calculating EKE requires wind data at a minimum of daily resolution and throughout the atmospheric column, and these data were only available for one model (IPSL-CM5A) for the G1, PI, and 4xCO₂ experiments. Therefore, in this study we use a metric of storm track intensity, extratropical cyclone activity (ECA), that instead requires surface pressure (psl) data, which were available for six models for the G1, PI, and 4xCO₂ experiments. ECA also has the advantage that as a surface metric it is more relevant for some impacts of extratropical cyclones.

Here we compare the changes in the extratropical storm track intensity as measured by ECA and EKE in the model for which sufficient data is available (IPSL-CM5A). To calculate EKE, we apply a 2.5-6-day Butterworth bandpass filter to daily horizontal winds from IPSL-CM5A. At each location, we calculate a mass-weighted vertical integral of kinetic energy to give the local vertically integrated EKE, and an area-weighted mean of EKE is then calculated over the extratropical latitude bands as an estimate of extratropical storm track intensity. We consider averages over the 30-70° latitude band, and we again use PI as the baseline when calculating the response to climate change.

Figure S13 shows that the changes in ECA and EKE are similar in the Southern Hemisphere, with large increases for 4xCO₂ and smaller decreases for G1, and in the Northern Hemisphere, with small decreases for 4xCO₂ and G1. It would be of interest to compare the behavior of ECA and EKE across a range of models and scenarios in future work.

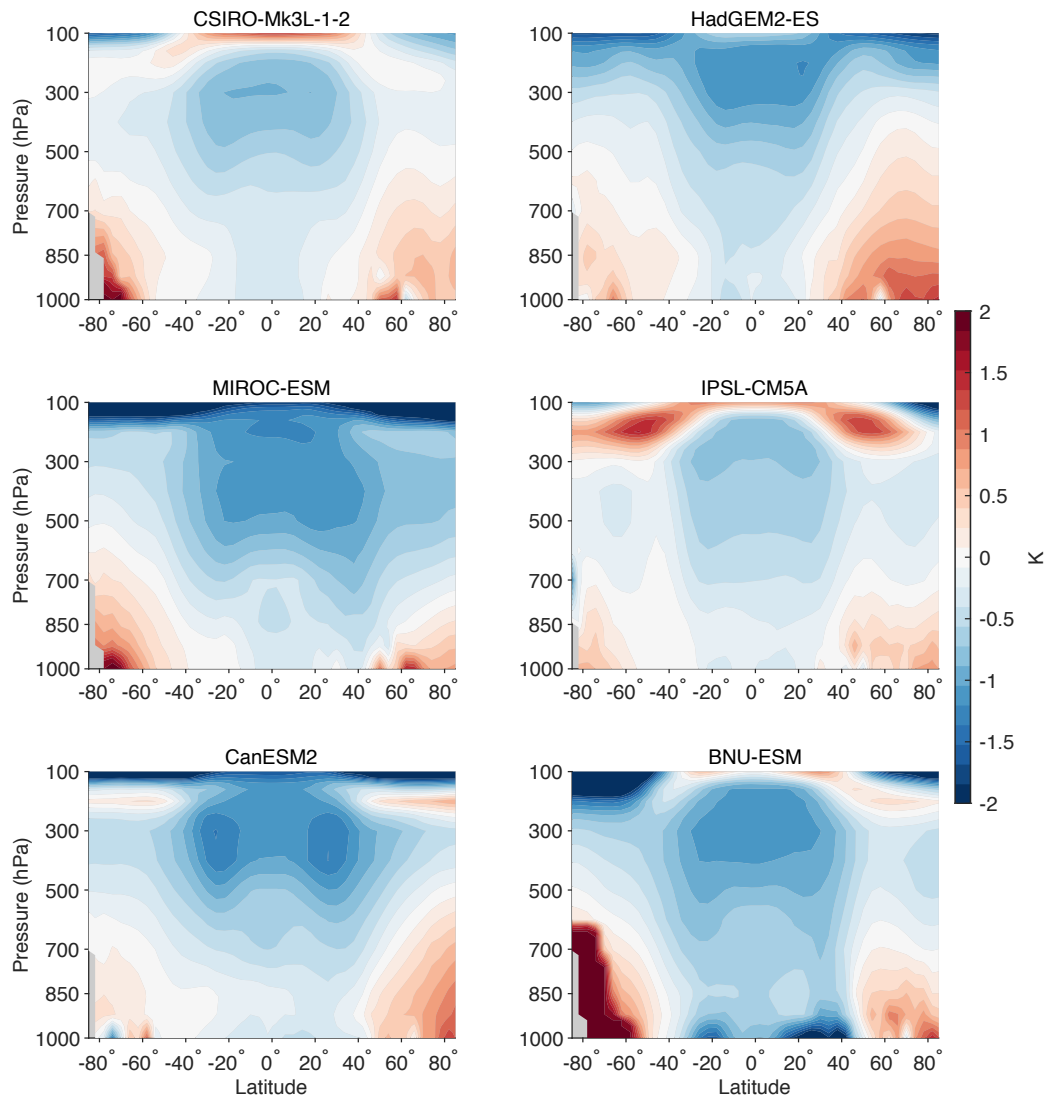


Figure S1. Zonal-mean temperature responses for G1 in individual models. The colorbar is saturated in some regions.

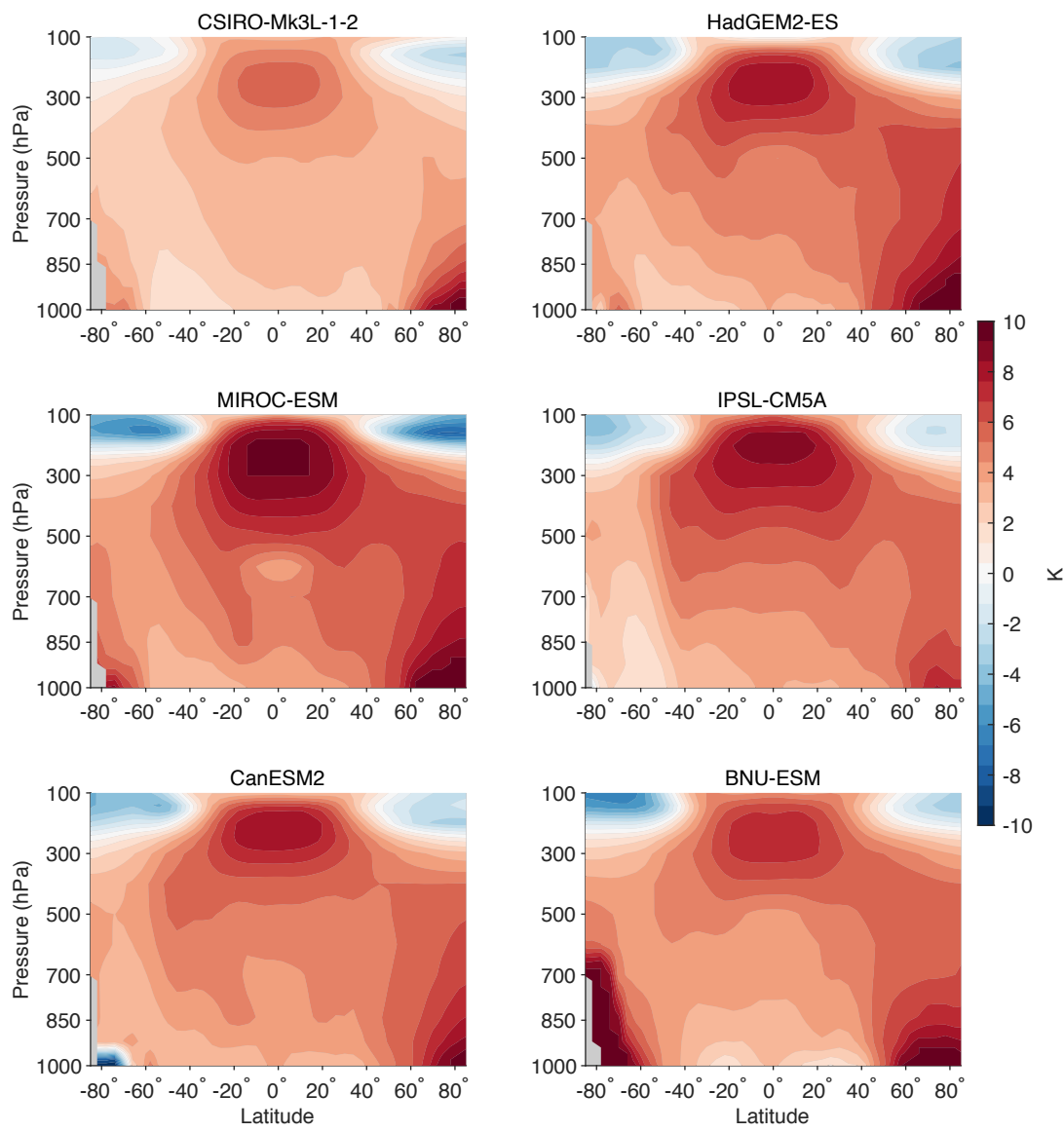


Figure S2. Zonal-mean temperature responses for 4xCO₂ in individual models.

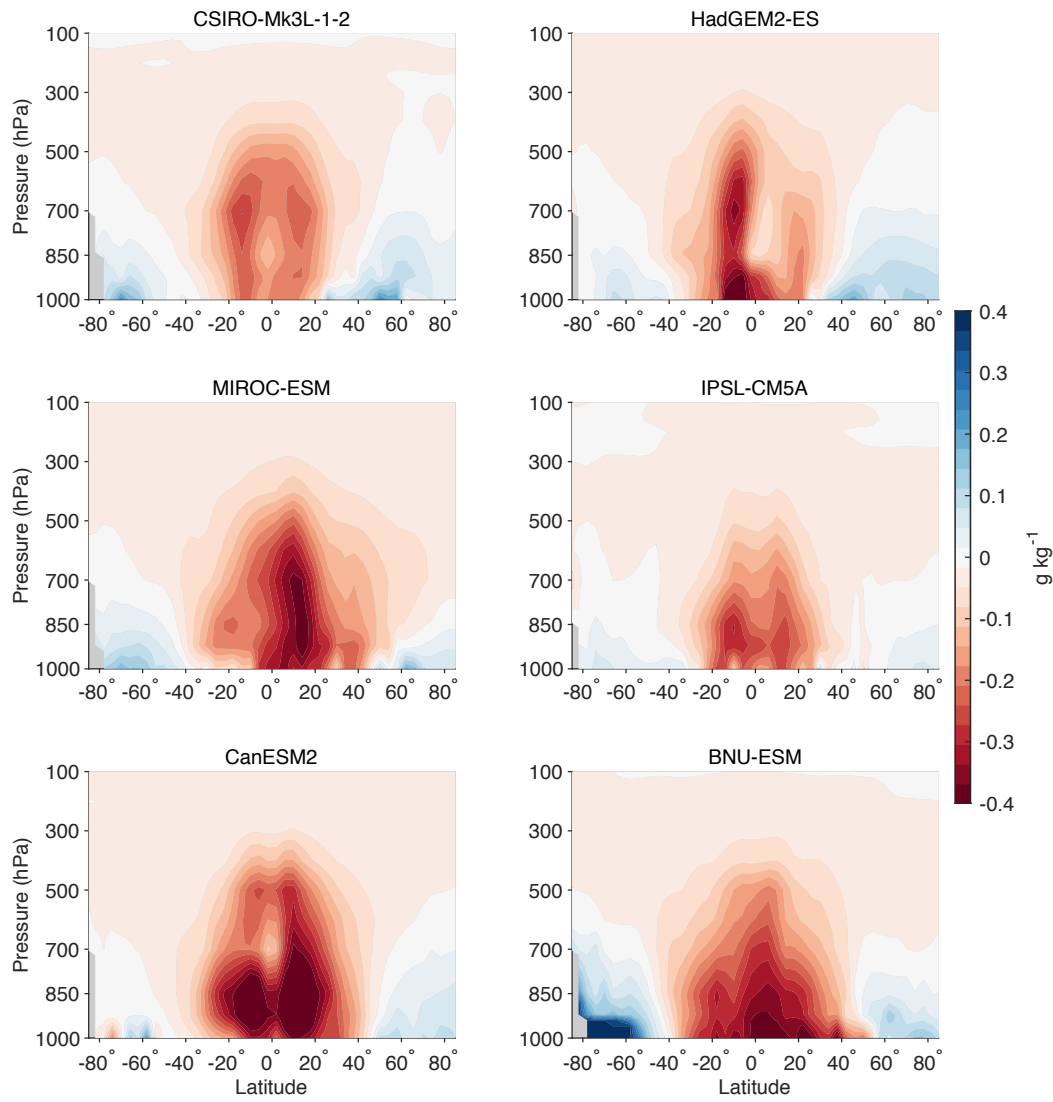


Figure S3. Zonal-mean specific humidity responses for G1 in individual models. The colorbar is saturated in some regions.

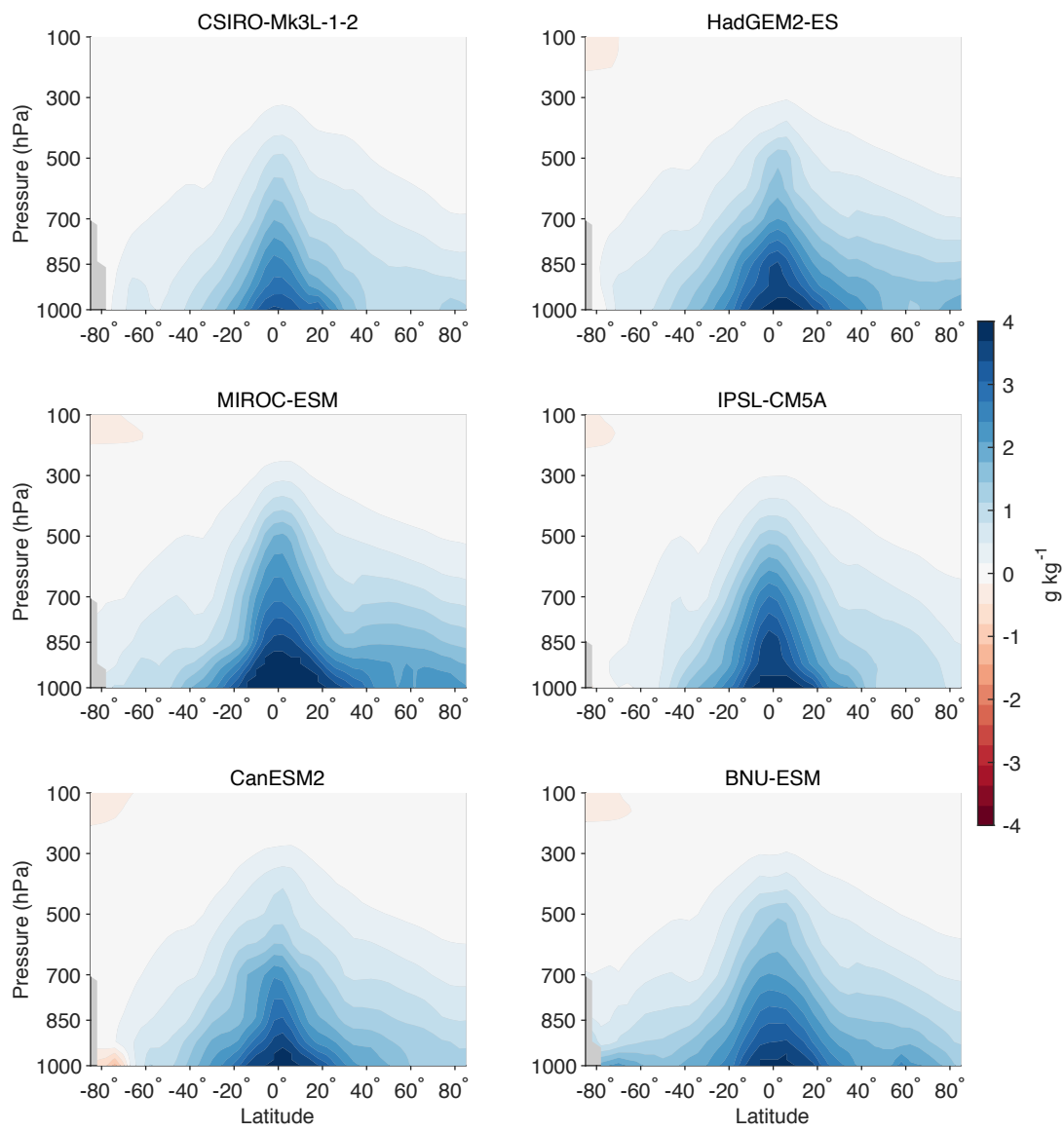


Figure S4. Zonal-mean specific humidity responses for $4\times\text{CO}_2$ in individual models.

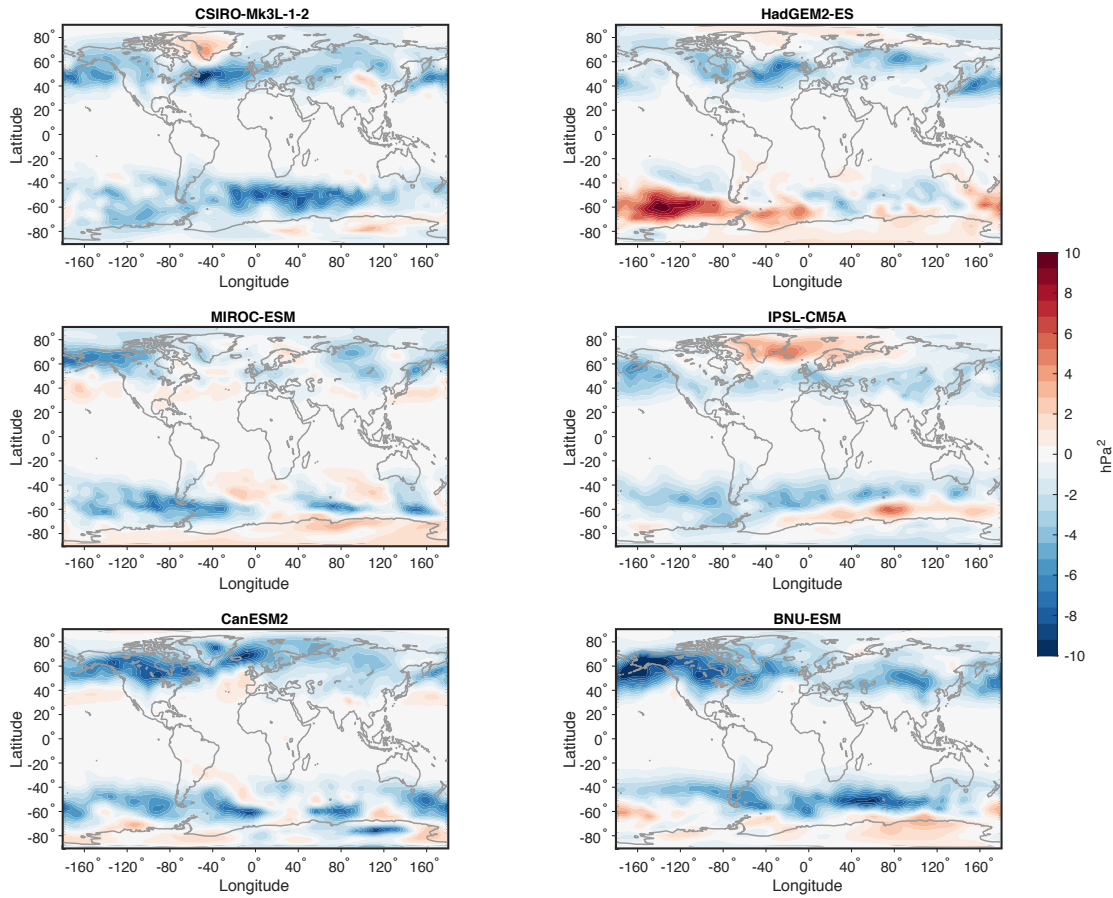


Figure S5. ECA responses for G1 in individual models.

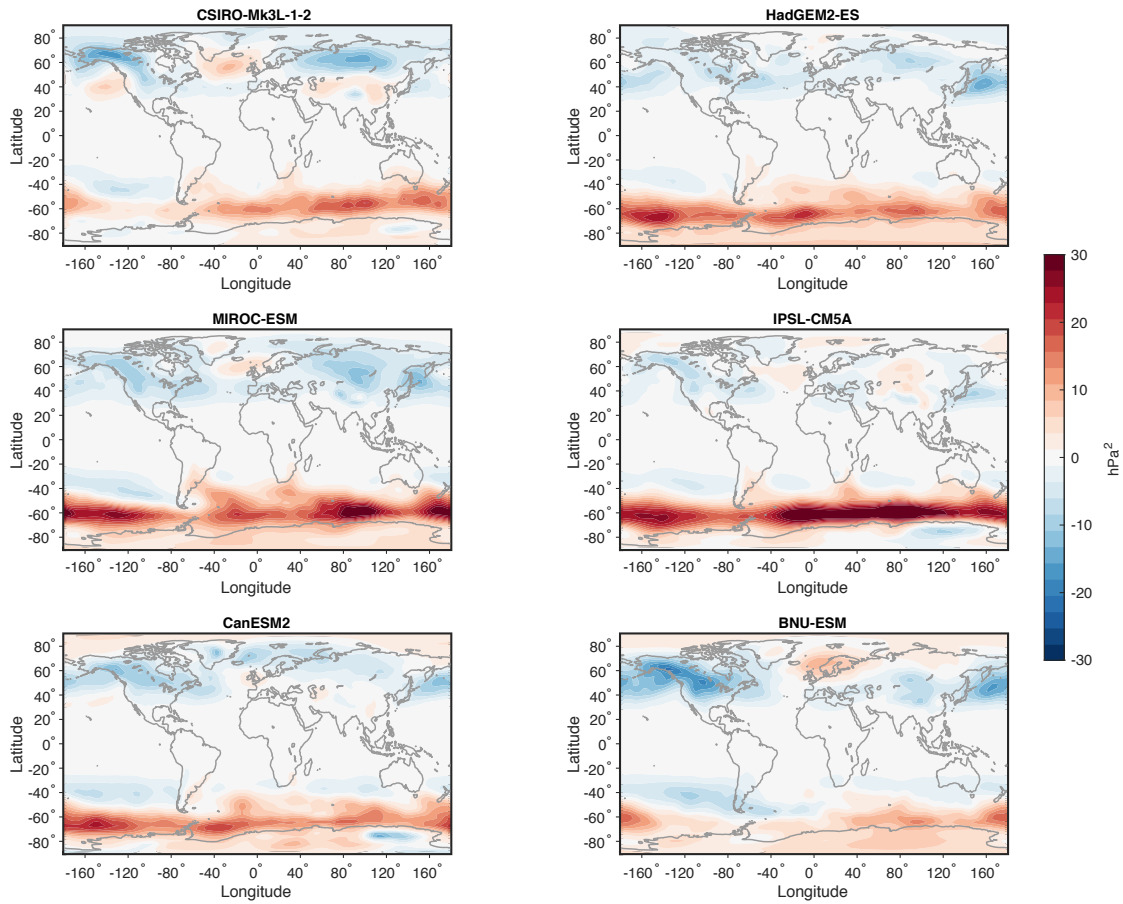


Figure S6. ECA responses for 4xCO₂ in individual models.

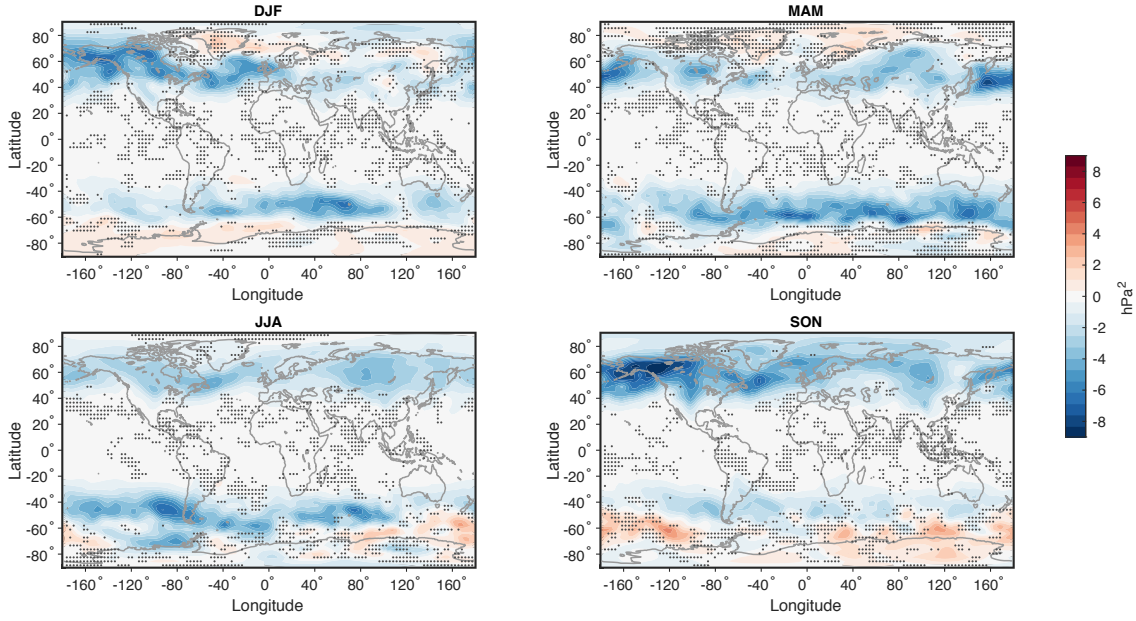


Figure S7: Model-mean ECA response for G1 in winter (DJF), spring (MAM), summer (JJA), and fall (SON). Stippling indicates regions where fewer than four of six models agree on the sign of the response.

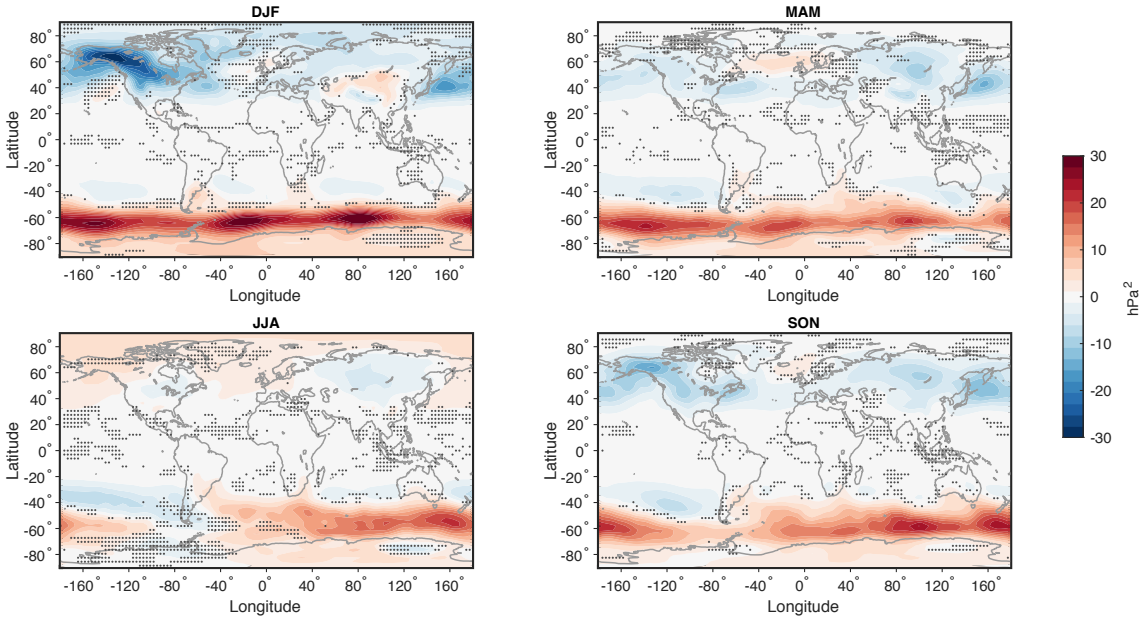


Figure S8: Model-mean ECA response for 4xCO_2 in winter (DJF), spring (MAM), summer (JJA), and fall (SON). Stippling indicates regions where fewer than four of six models agree on the sign of the response.

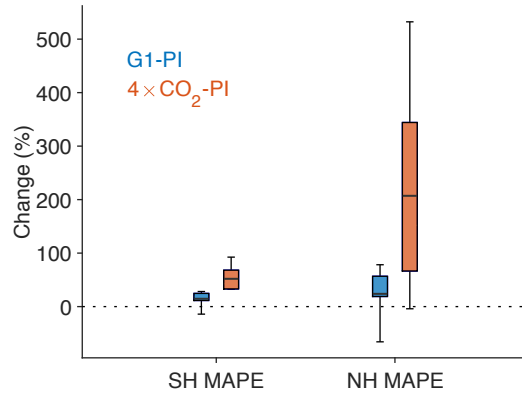


Figure S9. Fractional changes in convective MAPE for G1 (blue) and 4xCO₂ (red) in the Southern Hemisphere (SH) and Northern Hemisphere (NH). Box indicates range of inner 4 models (second and fifth sextiles), whiskers indicate maximum and minimum values, and mid-lines indicate model mean values. All MAPE values shown are calculated over 30–70° latitude.

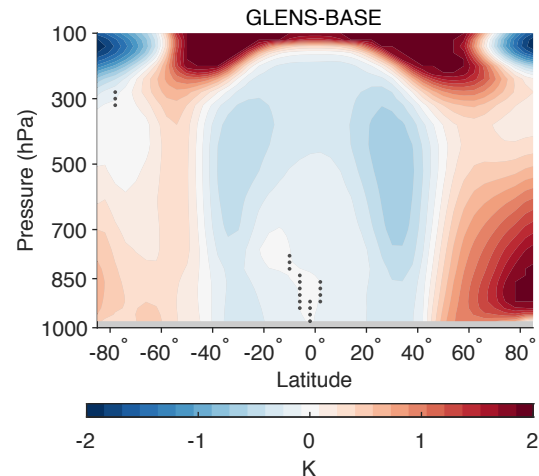


Figure S10: Ensemble- and zonal-mean temperature response for GLENS-BASE. Stippling indicates regions where fewer than two-thirds of ensemble members agree on the sign of the response. The colorbar is saturated in the lower stratosphere.

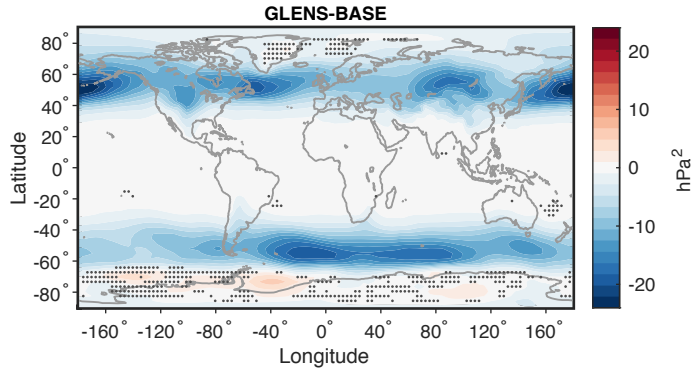


Figure S11: Ensemble-mean storm track intensity response for GLENS-BASE, as measured by ECA. Stippling indicates regions where fewer than two-thirds of ensemble members agree on the sign of the response.

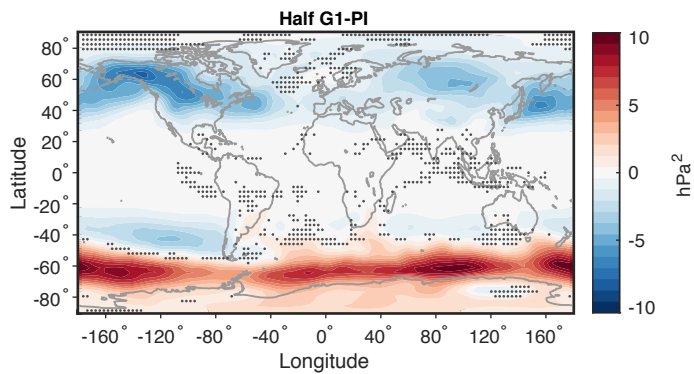


Figure S12: Model-mean storm track intensity response for “Half G1”, as measured by ECA. Stippling indicates regions where fewer than four of six models agree on the sign of the response.

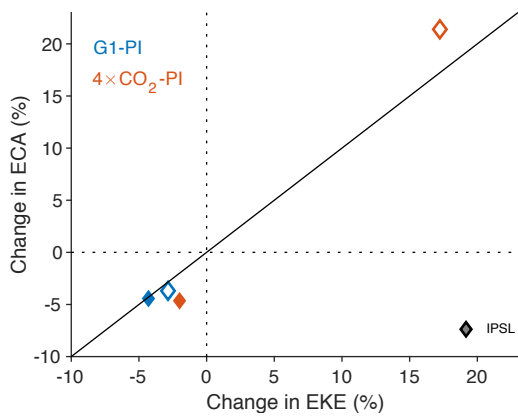


Figure S13. Changes in the IPSL-CM5A climate model for two different measures of extratropical storm track intensity. Shown are the fractional changes in ECA and EKE in experiment G1 (blue) and $4\times\text{CO}_2$ (red) for the Northern Hemisphere (filled symbols) and Southern Hemisphere (open symbols).

Model	Reference	Grid size (longitude x latitude x pressure)
MIROC-ESM	Watanabe et al. (2011)	128 x 64 x 35
IPSL-CM5A-LR	Dufresne et al. (2013)	96 x 96 x 17
HadGEM2-ES	Collins et al. (2011)	192 x 144 x 17
CSIRO-Mk3L-1-2	Phipps et al. (2011)	64 x 56 x 18
CanESM-2	Arora et al. (2011)	128 x 64 x 22
BNU-ESM	Ji et al. (2014)	128 x 64 x 17

Table S1. Climate models used for G1, 4xCO₂, and PI, their standard references, and the grid sizes of model output.

Experiment	NH ECA Change	NH MAPE Change	SH ECA Change	SH MAPE Change
4xCO ₂	-8.2%	-6.1%	9.8%	8.1%
G1	-5.2%	-4.3%	-2.6%	-2.7%
Half G1	-6.7%	-5.8%	2.0%	3.6%
GLENS	-16.9%	-14.6%	-6.3%	-8.1%

Table S2: Ensemble-average changes in ECA and nonconvective MAPE for all experiments compared to appropriate control experiments. For G1, 4xCO₂, and Half G1, the control experiment is PI. For GLENS, the control experiment in BASE.

References

- Arora, V. K., Scinocca, J. F., Boer, G. J., Christian, J. R., Denman, K. L., Flato, G. M., . . . Merryfield, W. J. (2011). Carbon emission limits required to satisfy future representative concentration pathways of greenhouse gases. *Geophysical Research Letters*, 38, L05805. doi:10.1029/2010gl046270
- Collins, W. J., Bellouin, N., Doutriaux-Boucher, M., Gedney, N., Halloran, P., Hinton, T., . . . Woodward, S. (2011). Development and evaluation of an Earth-System model-HadGEM2. *Geoscientific Model Development*, 4(4), 1051-1075. doi:10.5194/gmd-4-1051-2011
- Curry, C. L., Sillmann, J., Bronaugh, D., Alterskjaer, K., Cole, J. N. S., Ji, D. Y., . . . Yang, S. T. (2014). A multimodel examination of climate extremes in an idealized geoengineering experiment. *Journal of Geophysical Research: Atmospheres*, 119(7), 3900-3923. doi:10.1002/2013jd020648
- Dufresne, J. L., Foujols, M. A., Denvil, S., Caubel, A., Marti, O., Aumont, O., . . . Vuichard, N. (2013). Climate change projections using the IPSL-CM5 Earth System Model: from CMIP3 to CMIP5. *Climate Dynamics*, 40(9-10), 2123-2165. doi:10.1007/s00382-012-1636-1
- O'Gorman, P. A. (2010). Understanding the varied response of the extratropical storm tracks to climate change. *Proceedings of the National Academy of Sciences*, 107(45), 19176-19180. doi:10.1073/pnas.1011547107
- Phipps, S. J., Rotstayn, L. D., Gordon, H. B., Roberts, J. L., Hirst, A. C., & Budd, W. F. (2011). The CSIRO Mk3L climate system model version 1.0-Part 1: Description and evaluation. *Geoscientific Model Development*, 4(2), 483-509. doi:10.5194/gmd-4-483-2011
- Watanabe, S., Hajima, T., Sudo, K., Nagashima, T., Takemura, T., Okajima, H., . . . Kawamiya, M. (2011). MIROC-ESM 2010: model description and basic results of

CMIP5-20c3m experiments. *Geoscientific Model Development*, 4(4), 845-872.
doi:10.5194/gmd-4-845-2011